# Phase-separation transition in liquid mixtures near curved charged objects

Gilad Marcus,[1] Sela Samin,[2] and Yoav Tsori[2,a)]
[1]*Max-Planck-Institut für Quantenoptik, Hans-Kopfermann-Str. 1, D-85748 Garching, Germany*
[2]*Department of Chemical Engineering, Ben-Gurion University of the Negev, 84105 Beer-Sheva, Israel*

(Received 7 April 2005; accepted 10 July 2008; published online 8 August 2008)

We study the thermodynamic behavior of nonpolar liquid mixtures in the vicinity of curved charged objects, such as electrodes or charged colloids. There is a critical value of charge (or potential), above which a phase-separation transition occurs, and the interface between high- and low-dielectric constant components becomes sharp. Analytical and numerical composition profiles are given, and the equilibrium front location as a function of charge or voltage is found. We further employ a simple Cahn–Hilliard type equation to study the dynamics of phase separation in spatially nonuniform electric fields. We find an exponential temporal relaxation of the demixing front location. We give the dependence of the steady-state location and characteristic time on the charge, mixture composition and ambient temperature. © *2008 American Institute of Physics*.
[DOI: 10.1063/1.2965906]

Situations where charged objects, such as electrodes or colloids, are found in liquid environments are abundant in science and technology. In ionic mixtures, experiments and theory show that ions migrate toward the object and lead to screening of the electric field. In nonpolar liquids, the situation is different: the decay of electric field far from the objects depends on the geometry of all conducting surfaces and may be long range. When a nonpolar liquid mixture is under the influence of a uniform electric field $E$, the theories of Landau[1] and later Onuki[2] showed that the critical temperature can change by a small amount, proportional to $E^2$. Experiment by Debye and Kleboth[3] partially confirmed the theory.

However, here we show that the situation in spatially nonuniform electric fields, occurring when liquid mixtures are found under the influence of curved charged surfaces, is quite different. When the temperature $T$ is larger than the critical temperature $T_c$, the mixture exhibits smooth composition variations. This dielectrophoretic behavior is reminiscence of the effect of gravity.[4] For a homogeneous mixture below $T_c$, there are two scenarios: If the charge density is small, there are still weak composition gradients. On the other hand, large enough charge leads to a phase-separation transition, where the liquid with high-dielectric constant is close to the high field region while the liquid with low dielectric constant is pulled away, and the coexisting domains are separated by a sharp composition front.

The phase transition described below occurs in systems described by bistable free-energy functionals giving rise to a phase diagram in the composition-temperature plane divided into two regions: homogeneous mixture and a phase-separated state. In order to be specific and to facilitate the connection to experiment, we consider the following binary mixture free-energy density $f_m=kT\tilde{f}_m/Nv_0$, where

$$\tilde{f}_m = \phi \log(\phi) + (1-\phi)\log(1-\phi) + N\chi\phi(1-\phi). \qquad (1)$$

This symmetric ($N_A=N_B=N$) free energy is given in terms of the $A$-component composition $\phi$ ($0<\phi<1$) in a mixture of $A/B$ liquids, and the so-called Flory parameter $\chi\sim 1/T$.[5] Simple liquids have $N=1$, while polymers have $N>1$ monomers, each of volume $v_0$. $k$ is the Boltzmann constant. The critical point is given at $(\phi_c,(N\chi)_c)=(1/2,2)$. In the absence of electric field, the mixture is homogeneous if $T>T_t$, and unstable otherwise. The transition (binodal) temperature $T_t$ at a given composition is given by $T_t=(N\chi)_c T_c[\log(\phi/(1-\phi))/(2\phi-1)]^{-1}$.[5] The phase transition does not depend on the exact form of $f_m$, and appears in a Landau series expansion of Eq. (1) around $\phi_c$, or in any other similar "double-well" free-energy functional.

As is shown below, the effect of electric fields is large if they originate from curved charged surfaces. In this work we consider for simplicity surfaces with fixed curvature: a charged spherical colloid, a charged wire or two concentric cylinders, and the "wedge" capacitor, made up from two flat and nonparallel surfaces. Fixed charges on the conductors, fixed potentials, or a combination of the two are considered by us. When the mixture is in the vicinity of a charged object with a fixed surface charge, the total dimensionless free energy is $\tilde{f}=\tilde{f}_m+\tilde{f}_{es}$, where $\tilde{f}_{es}=(Nv_0/kT)[(1/2)\varepsilon(\phi)(\nabla\psi)^2]$ is the dimensionless electrostatic free-energy density.[1,6] Note that we do not include any direct short- or long-range interactions between the liquid and the confining walls.

The equilibrium state is a solution of the two coupled nonlinear equations: $\delta\tilde{f}/\delta\phi=0$ and $\delta\tilde{f}/\delta\psi=0$, where $\psi$ is the electrostatic potential obeying the proper boundary conditions.[2,7] The equation $\delta\tilde{f}/\delta\psi=0$ leads to Laplace's equation: $\nabla\cdot(\varepsilon(\phi)\nabla\psi)=0$, and is readily solved by the use of Gauss' law for systems with prescribed charges on the confining conductors and in azimuthal or spherical symmetries. For example, for a mixture confined between two infinite concentric cylinders of radii $R_1$ and $R_2>R_1$, we find $E$

a)Electronic mail: tsori@bgu.ac.il.

 

$=-\nabla\psi=\lambda/(2\pi\varepsilon(\phi)r)$, where $\lambda$ is the charge per unit length on the inner cylinder and $r$ is the distance from the cylinder's center. Subsequently, $\delta\tilde{f}_{es}/\delta\phi=-N^2v_0\chi/(kT_c)\times(\lambda/(4\pi\varepsilon r))^2 d\varepsilon/d\phi$. Similarly, $E=Q/(4\pi\varepsilon(\phi)r^2)$ for a spherical colloid of radius $R_1$ and charge $Q$, and $r$ is the distance from the colloid's center, and $E=V/(\beta r)$ for a wedge consisting of two flat conductors with potential difference $V$ and opening angle $\beta$ between them, and $r$ is the distance from the imaginary meeting point of the conductors.

We thus arrive at a considerable simplification of the problem, since the expression for $E$ obtained above allows to write a single dimensionless governing equation for all three cases with radial or azimuthal symmetry:

$$\log\left(\frac{\phi}{1-\phi}\right)+N\chi(1-2\phi)-N\chi M\frac{d\tilde{\varepsilon}/d\phi}{\tilde{\varepsilon}^2(\phi)}\tilde{r}^{-n}-\mu=0. \quad (2)$$

In the above, $M$ is the dimensionless ratio between the maximum electrostatic energy stored in a molecular volume and the thermal energy. $M$ is $M_c\equiv\lambda^2Nv_0/(16\pi^2kT_cR_1^2\varepsilon_0)$ for two concentric cylinders, $M$ is $M_s\equiv Q^2Nv_0/(64\pi^2kT_c\varepsilon_0R_1^4)$ for a spherical colloid, and $M$ is $\tilde{\varepsilon}^2M_w$ for the wedge, where $M_w\equiv V^2Nv_0\varepsilon_0/(4\beta^2kT_cR_1^2)$, $V$ is the voltage between the wedge plates, and $R_1$ is the smallest distance from the conductors' edge to their imaginary meeting point. $\tilde{r}\equiv r/R_1$ is the scaled distance from the center of the sphere or the inner cylinder, and $\tilde{\varepsilon}=\varepsilon/\varepsilon_0$, where $\varepsilon_0$ is the vacuum permittivity. Finally, $n$ is the exponent characterizing the fall of $E^2$: $n=2$ for concentric cylinders and the wedge geometries, and $n=4$ for the sphere. The importance of curvature is exemplified by the appearance of $R_1$ in the expressions for the $M$'s. $\mu$ is a Lagrange multiplier needed to conserve the average mixture composition: $\langle\phi(\mathbf{r})\rangle=\phi_0$, and $\phi_0$ is the average composition. In the case of an open system coupled to a particle reservoir at $r\to\infty$, $\mu$ is the reservoir's chemical potential. The phase transition described below is from a homogeneous (mixed) to a demixed state, and therefore it is assumed that $\phi_0$ is outsides of the binodal curve, namely, $T>T_t$.

Equation (2) expresses implicitly the composition profile $\phi(\tilde{r})$. Above $T_c$, $\phi(\tilde{r})$ has only smooth variations, irrespective of the value of $M$. Below $T_c$ [equivalently $N\chi>(N\chi)_c$], if $M$ is sufficiently small, the profile $\phi(\tilde{r})$ is smooth, with high-$\phi$ values at small $\tilde{r}$'s and low values at larger radii. However, there is a critical value of $M$, denoted $M^*$, above which $\phi(\tilde{r})$ exhibits a sharp jump: for $M>M^*$, high- and low-$\phi$ domains coexist separated by a clear interface at $\tilde{r}=\tilde{R}$. This transition occurs generally, even when the constitutive relation $\varepsilon(\phi)$ is linear in $\phi$. This is in contrast to the Landau mechanism, which relies on a quadratic dependence of $\varepsilon$ on $\phi$ and is responsible to a small change in $T_c$. We therefore chose the linear relation $\varepsilon(\phi)=\varepsilon_b+\phi\Delta\varepsilon$, where $\Delta\varepsilon\equiv\varepsilon_a-\varepsilon_b$, and $\varepsilon_a$ and $\varepsilon_b$ are the dielectric constants of components $A$ and $B$, respectively.

The typical demixing electric fields and surface or line charge density can be estimated from the values of $M$ (see Figs. 1 and 2). At $M_s=0.001$ and using a molecular volume of $Nv_0=10^{-26}$ m$^3$, colloid's radius $R_1=1$ $\mu$m, $T_c\simeq 300$ K, and $\tilde{\varepsilon}\simeq 4$, we find the electric field at the sphere's edge to be $E\sim 10^6-10^7$ V/m (surface potential $\sim 1-10$ V). The corresponding charge density is $\sigma=\varepsilon E\sim 10^{-5}-10^{-4}$ C/m$^2$ (total charge $Q=800-8000e$). Similar values for the electric field and charge density appear in the concentric cylinders and wedge geometries.

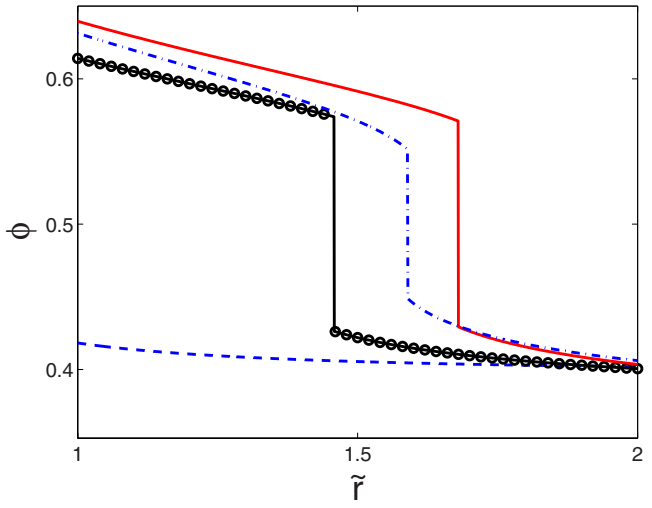


FIG. 1. (Color online) Equilibrium profiles $\phi(\tilde{r})$ for concentric cylinders with different dimensionless charge $M_c$. Dashed line: $T=0.991T_c$, and $M_c=0.008$ too small for phase separation. Circles: same $T$, but $M_c=0.04$. Solid line: same $T$, but $M_c=0.08$. Dash-dot line: $M_c=0.08$, but $T=0.994T_c$ is a higher temperature. We took fixed average composition $\phi_0=0.4$. In this and other figures, $\tilde{R}_1=1$, $\tilde{R}_2=5$, $\varepsilon_a=5\varepsilon_0$, and $\varepsilon_b=3\varepsilon_0$.

Figure 1 shows $\phi(\tilde{r})$ for a binary mixture confined by two concentric cylinders for several values of the dimension-

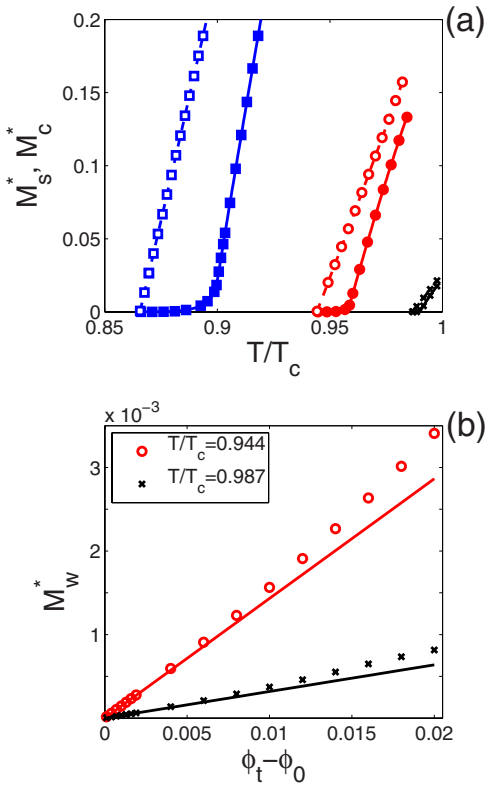


FIG. 2. (Color online) (a) Filled symbols: dimensionless critical charge $M_s^*$ for phase-separation near an isolated spherical colloid as a function of temperature. The colloid is coupled to a reservoir with three compositions: $\phi_0=0.2$ (squares), 0.3 (circles), and 0.4 (crosses). Open symbols: $M_c^*$ for a closed cylindrical system with same compositions. (b) $M_w^*$ vs $\Delta\phi=\phi_t-\phi_0$ from Eq. (3) (solid line) and from numerics (symbols).

less parameter $M_c$ and at two different temperatures. When $M_c=0.008$, there is no phase separation, and the profile is smooth. As $M_c$ increases above $M_c^*$, phase separation occurs, and $\phi(\tilde{r})$ rapidly changes from high to low values at the phase-separation front located at $\tilde{r}=\tilde{R}$. Further increase of $M_c$ at constant temperature leads to displacement of $\tilde{R}$ to larger values and to larger composition difference between coexisting domains.[8,9]

Figure 2(a) shows the calculated critical value $M_s^*$ as a function of temperature for a spherical colloid coupled to a particle reservoir at three different compositions. At a given $T$ above $T_t$, larger values of $|\phi_c-\phi_0|$ require more charge for demixing. Curves also show $M_c^*$ for a system enclosed between two concentric cylinders. Notice that approaching $T_t$, $M^*$ becomes infinitesimally small. For a wedge with average composition $\phi_0$ close to the transition composition $\phi_t$ at given temperature, we obtain the following approximation:

$$M_w^* = \frac{\phi_t-\phi_0}{4\Delta\tilde{\varepsilon}}\frac{T}{T_c}\frac{d^2\tilde{f}_m(\phi_t)}{d\phi^2}g(x), \tag{3}$$

where $x\equiv R_2/R_1$ and $g(x)=2(x^2-1)/(x^2-1-2\ln x)$. Figure 2(b) shows $M_w^*$ from this formula and compares it with a more accurate numerical solution.

We now turn to describe the relaxation toward equilibrium. The dynamics are governed by the following set of equations:[10–12]

$$\frac{\partial\phi}{\partial t}+\mathbf{u}\cdot\nabla\phi = L\nabla^2\delta f/\delta\phi, \tag{4}$$

$$\nabla\cdot(\varepsilon(\phi)\nabla\psi)=0, \tag{5}$$

$$\nabla\cdot\mathbf{u}=0, \tag{6}$$

$$\rho\left[\frac{\partial\mathbf{u}}{\partial t}+(\mathbf{u}\cdot\nabla)\mathbf{u}\right]=\eta\nabla^2\mathbf{u}-\nabla P-\phi\nabla\,\delta f/\delta\phi, \tag{7}$$

where $\mathbf{u}$ is the velocity field corresponding to hydrodynamic flow and $\eta$ is the liquid viscosity. Equation (4) is a continuity equation for $\phi$, where $-L\nabla(\delta f/\delta\phi)$ is the diffusive current due to the inhomogeneities of the chemical potential, and $L$ is the transport coefficient (assumed constant). Equation (5) is Laplace's equation, Eq. (6) implies incompressible flow, and Eq. (7) is Navier–Stokes equation with a force term $-\phi\nabla\,\delta f/\delta\phi$.[12]

We continue in the limit of overdamping and with the assumption of azimuthal symmetry. It follows that $\mathbf{u}=0$. We use the dimensionless time $\tilde{t}=Nv_0R_1^2t/(LkT)$, radius $\tilde{r}=r/R_1$, and energy $\tilde{f}=Nv_0f/kT$, to express $\phi$ as a solution to a diffusionlike equation $\partial\phi/\partial t=\nabla^2\delta f/\delta\phi$, while satisfying Laplace's equation, where the "~" signs have been omitted for brevity of notation. The time dependence of the profile $\phi(\tilde{r},t)$, obtained numerically, is shown in Fig. 3 for several times $t$.

The dimensionless location of the demixing front changes as a function of time: $\tilde{R}=\tilde{R}(t)$ and asymptotically tends toward the steady-state front location $\tilde{R}_\infty$ at long times.

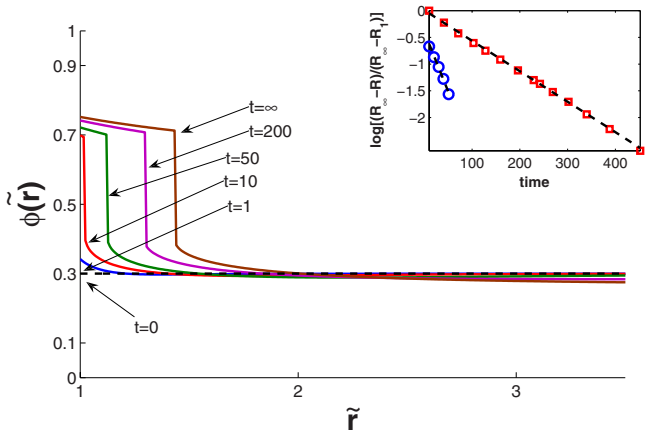


FIG. 3. (Color online) Composition profiles $\phi(\tilde{r},t)$ at several dimensionless times for concentric cylinders with $M_c=0.32$, $\phi_0=0.3$, and $T=0.95T_c$. Inset: semilog plot of $\tilde{R}(t)$. Numerical results (squares) and experiments of Ref. 7 (circles, time in s).

We find excellent match with an exponential relaxation of the form $\tilde{R}(t)=\tilde{R}_\infty+(1-\tilde{R}_\infty)\exp(-t/\tau)$, as is shown in the inset of Fig. 3.

Figure 4 shows the location of the steady-state demixing front $\tilde{R}_\infty$ and the time constant $\tau$ at several different values of $\phi_0$ and $T$, and for two different values of $M_c$. It is worth noting that all the points with the same $M_c$ seem to fall on the same line. Similarly, the dependence of $\tilde{R}_\infty$ on $\phi_0$ is displayed in Fig. 5(a). Clearly, the domain size increases with $M_c$ at constant temperature and composition. Increase of $\phi_0$ at constant $T$ and $M_c$ increases the domain size. Figure 5(b) shows how $\tau$ depends on $\phi_0$. Compositions closer to $\phi_c$ exhibit slower relaxations. In addition, increase of $M_c$ leads to faster relaxation toward steady state.

It should be emphasized that this phase transition is not restricted to the vicinity of the critical point, and it occurs at all compositions, provided that the electric field is large enough. Moreover, field-induced prewetting could also be

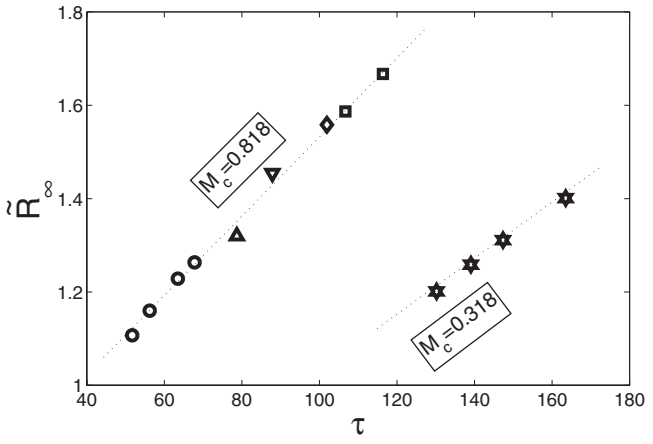


FIG. 4. Steady-state front location $\tilde{R}_\infty$ vs time constant $\tau$ for different temperatures and compositions. Stars: $M_c=0.318$, $\phi_0=0.3$ and $0.95\leqslant T/T_c\leqslant 0.99$. Circles: $M_c=0.818$, $\phi_0=0.2$, and $0.89\leqslant T/T_c\leqslant 0.95$. Squares: $M_c=0.818$, $\phi_0=0.3$, and $0.95\leqslant T/T_c\leqslant 0.97$. Up and down triangles and diamond: $\phi_0=0.22$, $\phi_0=0.24$, and $\phi_0=0.26$, respectively, $M_c=0.818$ and $T/T_c=0.95$.

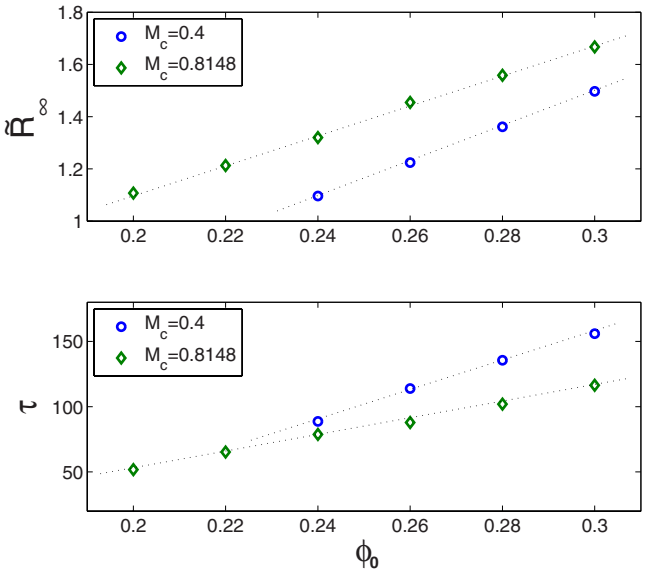


FIG. 5. (Color online) Steady-state front location $\tilde{R}_\infty$ (a) and time constant $\tau$ (b) vs $\phi_0$ for two values of dimensionless charge $M_c$. Numerical solution for concentric cylinders with $\tilde{R}_1=1$, $\tilde{R}_2=5$, and $T=0.95T_c$.

realized in vapor-liquid systems of pure substances subject to nonuniform electric fields.

There are several circumstances where the field-induced separation may have an important influence. Colloidal suspension in liquid mixtures and polymer solutions have been extensively studied.[13–17] We point out that standard wetting theory is insufficient to describe these experiments if the colloids are charged. The enrichment layer around the colloid is sensitive to the colloid's charge, and this may have an effect on the intercolloid interaction and hence on the phase behavior and the rheology of suspensions.[16,17]

A drastic change to the rheological properties is also predicted for a mixture confined, for example, between two rotating coaxial cylinders (Taylor–Couette flow). The classic (zero field) flow profile would change markedly if a potential is imposed between the two cylinders. Once the homogeneous mixture demixes, most of the velocity gradient will fall on the liquid component with smaller viscosity.[18] A change to the lubrication in microelectromechanical systems and in microfluidic channels can be similarly brought by the application of external potential, recalling that in these systems the electric field is inherently nonuniform.

Last, we point out that the demixing transition creates optical interfaces, since the mixture's components have different refraction indices. Consequently, the propagation of a light beam through a mixture in a channel will be altered once an electric field creates optical interfaces, and this may be used to scatter, focus, or even guide rays in microfluidic arrays.[19]

We thank L. Leibler and F. Tournilhac for help in developing the ideas presented in this work, and D. Andelman for numerous useful comments. This research was supported by the Israel Science Foundation (ISF) Grant No. 284/05, and by the German Israeli Foundation (GIF) Grant No. 2144-1636.10/2006.

[1] L. D. Landau and E. M. Lifshitz, *Elektrodinamika Sploshnykh Sred* (Nauka, Moscow, 1957), Chap. II, Sec. 18, Problem 1.
[2] A. Onuki, Europhys. Lett. **29**, 611616 (1995).
[3] P. Debye and K. Kleboth, J. Chem. Phys. **42**, 3155 (1965).
[4] M. R. Moldover, J. V. Sengers, R. W. Gammon, and R. J. Hocken, Rev. Mod. Phys. **51**, 79 (1979).
[5] M. Doi, *Introduction to Polymer Physics* (Oxford University Press, Oxford, UK, 1996).
[6] A. Onuki and H. Kitamura, J. Chem. Phys. **121**, 3143 (2004).
[7] Y. Tsori, F. Tournilhac, and L. Leibler, Nature (London) **430**, 544 (2004).
[8] K. Y. C. Lee, J. F. Klinger, and H. M. McConnell, Science **263**, 655 (1994).
[9] Y. Tsori and L. Leibler, C. R. Phys. **8**, 955 (2007).
[10] T. Imaeda, A. Furukawa, and A. Onuki, Phys. Rev. E **70**, 051503 (2004).
[11] H. Tanaka, J. Phys.: Condens. Matter **12**, R207 (2000).
[12] A. J. Bray, Adv. Phys. **51**, 481 (2002).
[13] E. J. Meijer and D. Frenkel, J. Chem. Phys. **100**, 6873 (1994).
[14] D. G. A. L. Aarts, R. Tuinier, and H. N. W. Lekkerkerker, J. Phys.: Condens. Matter **14**, 7551 (2002).
[15] R. G. Larson, *The Structure and Rheology of Complex Fluids* (Oxford University Press, Oxford, 1999); D. F. Evans and H. Wennerström, *The Colloidal Domain: Where Physics, Chemistry, Biology and Technology Meet* (Wiley-VCH, New York, 1999).
[16] D. Beysens and T. Narayanan, J. Stat. Phys. **95**, 997 (1999).
[17] C. Hertlein, L. Helden, A. Gambassi, S. Dietrich, and C. Bechinger, Nature (London) **451**, 172 (2008).
[18] Y. Tsori and L. Leibler, Proc. Natl. Acad. Sci. U.S.A. **104**, 7348 (2007).
[19] D. Psaltis, S. R. Quake, and C. Yang, Nature (London) **442**, 381 (2006).